Dyes and Pigments 185 (2021) 108887

Contents lists available at ScienceDirect

Dyes and Pigments

journal homepage: http://www.elsevier.com/locate/dyepig

A combined experimental and DFT investigation of mono azo thiobarbituric acid based chalcone disperse dyes

Alaa Z. Omar [a,*], Mona N. Mahmoud [a], Samir K. El-Sadany [a], Ezzat A. Hamed [a], Mohamed A. El-atawy [a,b]

[a] Chemistry Department, Faculty of Science, Alexandria University, P.O. 426 Ibrahemia, Alexandria, 21321, Egypt
[b] Chemistry Department, Faculty of Science, Taibah University, Yanbu, 46423, Saudi Arabia

ARTICLE INFO

Keywords:
Disperse dye
Azo dye
Thiobarbituric acid
Chalcone
DFT
Fastness properties

ABSTRACT

A number of monoazo dyes were synthesized by the reaction of 4-aminoacetophenone with different substituted benzaldehydes to give a new series of chalcone derivatives. The diazonium salts of these chalcones then allowed to react with thiobarbituric acid to produce the appropriate azo dye. The structures of the newly synthesized dyes were assigned by IR, NMR spectral data. IR study confirmed the existence of azo-dioxothioxo tautomer in the solid phase while ^{1}H NMR study indicated the predominance of azoenol-oxothioxo or hydrazo-dioxothioxo tautomers. The geometries of the azo and hydrazo tautomeric forms and their electronic absorption of the dyes were optimized at B3LYP/6-311G level of theory. All the azo compounds were evaluated for their dyeing performance on polyester fibers, and PET. All the synthesized dyes gave moderate to excellent fastness properties on PET fiber. The effects of the nature of the substituents on the color and dyeing properties of these dyes have been evaluated. The mechanism of dyeing polyester fiber was discussed.

1. Introduction

The synthetic colors are widely applied in many fields of modern industries, such as textiles, leather, paper and in the production of food and hair dye [1]. The most common synthetic azo dyes used for dyeing fabrics and textiles were usually strongly colored due to π-delocalization i.e. the color intensity as well as the interaction of azo dyes with fibers depend on the structure of dyes and the dyed materials [2–7]. Disperse dyes contain azo chromophore are substantially water-insoluble i.e. non-ionic dyes and generally applied to hydrophobic fibers e,g, polyester, cellulose acetate, and nylon [8].

It has been reported that the introduction of the chalcone group to the azo compound will increase the conjugation and gave brighter hues on acetate, nylon and polyester fibers [3] but they didn't applicable on cotton fiber. It has been found that thiobarbituric acid derivatives have more pharmacological activity due to the presence of sulphur. Because of the simple application and of the acid character, the thiobarbiturates were used as valuable reagents in organic syntheses of biological activity [9–11] such as antiallergic [12], antifungal [13,14], antibacterial, antichlamydial, antiviral and immunomodulating activity [15,16] and antitumor agent [17].

The C_5–H bond in thiobarbituric acid is sufficiently acidic where in presence of base, it couples with diazonium salts, most often aqueous sodium acetate [18]. Azo colorants containing amino and hydroxyl substituents ortho or para to the azo groups can exist as a mixture of azo and hydrazo tautomers. While azo–hydrazo tautomers are quite interesting from a theoretical viewpoint as the two tautomers have different technical properties [18]. The aim of the present study is attempting to design azo thiobarbituric acid based chalcone derivatives with some application to dye fiber and predict the mechanism of dyeing if any. The study will extend to compute the absorption of the synthesized dyes using the Density Functional Theory (DFT).

2. Results and discussion

2.1. Chemistry

The chalcones azo thiobarbituric acid derivatives were synthesized by condensation of 4-aminoacetophenone **1** with some arylaldehyde **2a-k** to give 1-(4-aminophenyl)-3-arylprop-2-enone **3a-k,** followed by

* Corresponding author.
E-mail addresses: Alaazaki@alexu.edu.eg (A.Z. Omar), mona.nabih@alexu.edu.eg (M.N. Mahmoud), Samir.elsadany@alexu.edu.eg (S.K. El-Sadany), ezzat.awad@alexu.edu.eg (E.A. Hamed), mohamed.elatawi@alexu.edu.eg (M.A. El-atawy).

https://doi.org/10.1016/j.dyepig.2020.108887
Received 19 May 2020; Received in revised form 31 August 2020; Accepted 24 September 2020
Available online 28 September 2020

diazotization which then coupled with thiobarbituric acid to give the water insoluble disperse dyes Chalcone Azo Thiobarbituric acid (CAT) **4a-k,** Scheme 1.

As reported earlier [18], CAT dyes **4a-k** can exist in three main tautomeric forms, namely CAT azo-dioxothioxo tautomer **I**, CAT hydrazo-dioxothioxo tautomer **II** and CAT azo-enol-oxothioxo tautomer **III** as shown in Scheme 2. Tautomerism is not only important to chemists but also to the dyestuff manufacturer. Tautomers not only have different colors, but also have different properties, e.g. light fastness.

The FT-IR spectra of CAT dyes **4a-k** showed two intense carbonyls (C═O) peaks at 1666-1651 and 1712-1705 cm^{-1} (see experiment), while the hydroxyl group peak of the thiobarbituric moiety disappeared. Therefore, IR results suggest that the CAT dyes **4a-k** in the solid phase are predominantly exist in either azo-dioxothioxo tautomer **I** or CAT hydrazo-dioxothioxo **II** rather than CAT azo-enol-oxothioxo **III** tautomers, Scheme 2. On the other hand, the absence of peaks attributable to imino group (C═N) while the presence of weak peaks at υ cm^{-1} 1519-1496 for azo group (N═N) [19] excluded the CAT hydrazo-dioxothioxo tautomer **II** and suggests that the solid phase of dyes **4a-k** exist as CAT azo-dioxothioxo tautomer **I**. The FT-IR spectra also showed peaks at υ cm^{-1} 3471-3109, assigned to NH group, 3079-3000 cm^{-1} assigned to aromatic C–H, while aliphatic C–H peaks appear at υ cm^{-1} 2924–2862. The intense peaks at υ cm^{-1} 1350–1334 cm^{-1} correspond to thiocarbonyl (C═S).

Inspection of the ^{1}H NMR spectra of CAT dyes **4a-4c** and **4f-4j** showed the existence of two exchangeable broad singlet signals in the downfield region; one resonates in the range δ 12.5–12.54 ppm is attributed to two NH protons at the 1-position and 3-position of the thiobarbituric acid moeity. While, the more deshielded proton in the range δ 14.17–13.98 ppm, was attributed to one OH proton that forms hydrogen bonding with the azo group. Also, the absence of a signal for the methine proton (CH) suggests the existence of CAT dyes **4a-4c** and **4f-4j** in the azo-enol-oxothioxo tautomer **III**. While, ^{1}H NMR spectra of CAT dyes **4d-4e** and **4k** exhibit only one exchangeable broad singlet signal in the range δ 12.88–12.80 ppm attributed to three NH protons, indicating that these dyes exist in hydrazo-dioxothioxo tautomer **II**. The low-field broad singlet peaks of NH protons for all synthesized dyes, **4a-k** is presumably due to intramolecular hydrogen bond between carbonyl groups and NH of hydrazo-dioxothioxo tautomer **II** or between azo and OH of azo-enol-oxothioxo tautomer **III**, Fig. 3.

The methyl groups of compounds **4f** and **4j** were displayed in ^{1}H NMR at δ 2.36 and 2.44 ppm, respectively, while their ^{13}C APT NMR exhibited signals at δ 20.93 and 19.37 respective to their methyl carbon atoms. The methoxy and thiomethoxy groups in compounds **4g** and **4h** were appeared more deshielded singlet signals at δ 3.82 and 2.52 ppm in ^{1}H NMR spectra, while their ^{13}C APT-NMR spectra signals appeared at δ 55.41 and 14.17 ppm. Dye **4k** showed a triplet and two doublets signals at δ 7.19 and 7.79 ppm corresponding to aromatic protons in the thiophene ring.

The ^{1}H NMR spectra of CAT dyes **4a-k** show characteristic two doublet signals for α, β-protons which coalesced with aromatic protons. Obviously, in all cases the doublet for CH_{β} appeared around δ 8.02–7.60 ppm, which more deshielded than CH_{α} refers to the effect of adjacent phenyl ring that bonded to β-carbon atom. The doublet in the region δ 8.02–7.60 ppm with J coupling constant 14.6–15.6 Hz to H-β, indicates that the ethylene moiety in the enone linkage is in the *trans*-conformation. The optimized **4a**, geometry as well as 0° dihedral angle of Hα-C═C-Hβ stated that Hα and Hβ are existing in the *s-trans* conformation as suggested from ^{1}HNMR study [20].

R. E. Stuckey reported that the thiobrbituric acid may be characterized by equilibrium among thiobarbituric acid in monoenol-oxothioxo, dienol-thioxo and thiodienol tautomers [21,22]. Actually, the ^{1}H NMR measurements indicate that the synthesized dyes exist in thioldioxo **IV**, enolthioloxo **V** and dienolthiol tautomers **VI** are rejected, Fig. 1, and CAT dyes **4a-4c** and **4f-4j** exist in the azo-enol-oxothioxo tautomer **III** while dyes **4d-4e** and **4k** exist in hydrazo-dioxothioxo tautomer **II,** Scheme 2.

2.2. Electronic Absorption Spectra and substituent effect

The computational results of absorptions and the observed colors of mono azo disperse CAT dyes **4a-k** are compared with the experimental ones. The color strength values of dyeing process associated with some molecular descriptors are examined.

The computed absorption values of compounds **4a-k** using B3LYP/6-311G are ranged in the region of (403–427 nm) which nearly lie in the region of violet color absorption (400–435 nm), whereas, the observed color was yellow and yellowish-orange, Table 1.

The data in Table 1 shows that CAT dyes **4b-k** have slight shift in λ_{max} than the unsubstituted one **4a**, Fig. 2. This indicates that the positions of absorption bands are slightly dependent of the nature and position of the substituent on the aryl group of the chalcone moiety. Also, Table 1 showed that the computed absorption values of compounds **4a-k** (403–427 nm) are quit similar values compared with the experimental ones.

Each of the CAT dyes **4a-k** gave two absorption bands in the region λ nm 274.65–342.88 and 430.96–439.65 nm. These absorption bands mainly originate from the π →π* electronic transition involving the π-electron system of the molecule and n →π* from ground to excited state, respectively. Except, dye **4h** and **4k** have only one absorption bands at λ 437.48 and 436.24 nm, respectively, mainly are due to n →π* transition.

Examination of the results reported in Table 1, reveals that the introduction of either electron-donating or electron-withdrawing of the aryl ring containing chalcone moiety result in bathochromic shifts for both absorption bands compared to the unsubstituted dye **4a** (Ar =

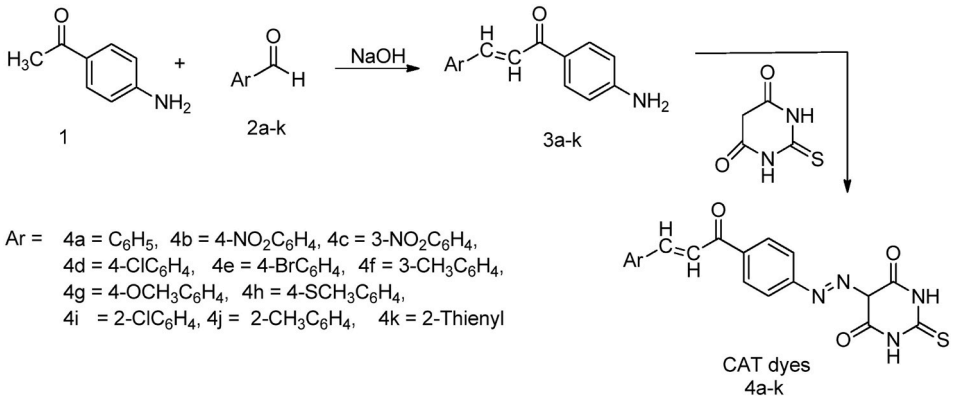

Scheme 1. Synthetic pathway of CAT dyes **4a-k**.

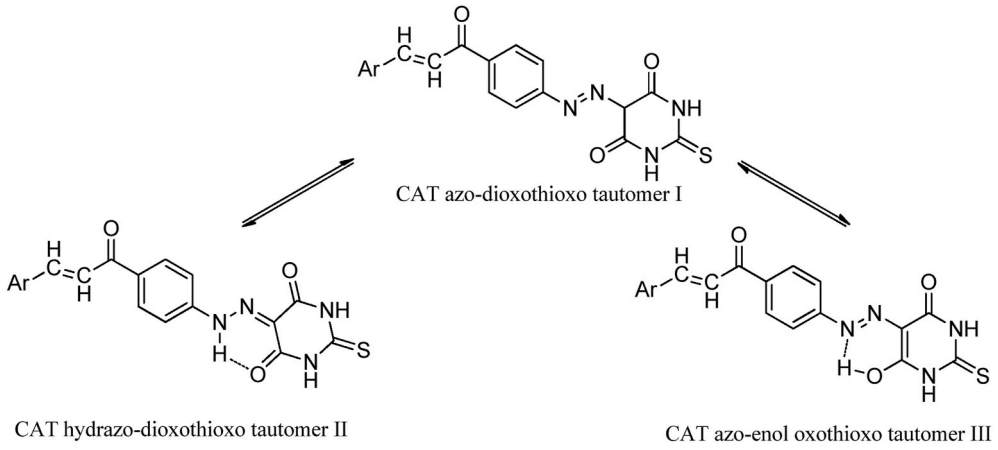

Scheme 2. Possible tautomeric form of CAT dyes **4a-k**.

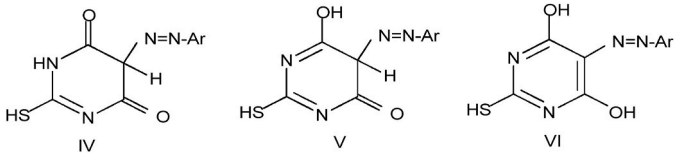

Fig. 1. Different tautumeric form of thiobarbituric acid moiety.

C_6H_5). The bathochromic shift can be attributed to more conjugation by introducing a substituent with different nature and position, except, dye **4i** (Ar = 2-ClC_6H_4) shows hypsochromic shifts for π →π* band, dyes **4e** (Ar = 4-BrC_6H_4) and **4g** (Ar = 4-$CH_3OC_6H_4$) exhibit hypsochromic shift for n →π* and whereas dye **4c** (Ar = 3-$NO_2C_6H_4$) shows hypsochromic shifts for both bands, Fig. 2.

2.3. Acidochromic effects

The presence of basic nitrogen atom of azo group, and an acidic tautomeric proton in the pyrimidine ring in the dyes **4a-k** prompted us to study the possibility of protonation and deprotonation of these CAT dyes in DMF, by using 0.1 M hydrochloric acid and 0.1 M sodium hydroxide Figs. 3 and 4, respectively. The effects of the acid and base on the absorption maxima of the dye solutions s are shown in Table 1. It shows that the absorption of the dyes in DMF are quite sensitive to pH change.

The absorption maxima of the CAT azo dyes **4a-k** in DMF showed bathochromic shift due to deprotonation upon addition of NaOH s, that leads to increase in donor-acceptor interplay between the enolate functionality and the chalcone moiety (the anionic form for dye **4a-k**). While, addition of hydrochloric acid to dye solutions in λ_{max} showed slight hypsochromic shifts. This is because protonation of azo group causes isolation the donor-acceptor interplay between chalcone and thiobarbituric moiety, Scheme 3.

2.4. Fastness properties

Washing, perspiration, scorch and light fastness have been done by using standard procedure [23,24], The physical data for the dyed polyester fibers were collected in Table 2. Wash fastness property depends mainly upon the solubility of dye in water and what type of linkage present between the dye molecule and fabrics whereas light fastness is the degree to which a dye resists fading due to light exposure. Scorch fastness is the most significant requirement of the dyed polyester fabrics, as the migration of the dye molecules of disperse dyes to polyester fabrics are totally dependent on the heat treatment. All of measured properties were assessed with gray scale from 1—poor to 6—excellent [25].

The fastness ratings show that the disperse CAT dyes (**4a-4c** and **4e-4k**) displayed good to very good fastness levels to washing, this is because of these dyes are hydrophobic, so high washing fastness ratings are expected. CAT dyes (**4a-4c** and **4e-4k**) exhibited moderate fastness levels to perspiration and very good fastness levels to scorch and light fastness.

2.5. Dye exhaustion

The uptake of our disperse azo dyes by fiber polyester was measured by sampling the dye bath before and after the dyeing [26]. The concentration (g/l) of the dye bath was measured on (pg instruments T80+) UV/visible spectrophotometer at λ_{max} of the corresponding dye. The percentage of the individual dye exhaustion on PET (% E) was calculated

Table 1
Experimental and computed absorption maxima of CAT dye 4a-k in DMF, DMF/0.1 M NaOH and DMF/0.1 M HCl.

Dye no.	Ar	Observed color	DMF λ (nm)		λ (nm)	
			Experimental	Computational	DMF + NaOH	DMF + HCl
4a	C_6H_5	yellow	308.76, 435.00	408.43	309.07, 464.77	314.66, 424.76
4b	4-NO_2 C_6H_4	orange	317.14, 430.96	403.60	318.07, 446.47	319.62, 424.76
4c	3-NO_2 C_6H_4	orange	274.65, 432.51	409.49	274.65, 447.09	276.20, 423.52
4d	4-Cl C_6H_4	orange	310.03, 439.65	427.18	310.62, 467.25	318.07, 423.83
4e	4-Br C_6H_4	yellow	315.59, 434.37	409.05	313.73, 465.70	319.31, 425.07
4f	3-CH_3 C_6H_4	orange	310.62, 437.43	410.77	312.49, 465.08	315.59, 424.76
4g	4-OCH_3 C_6H_4	yellow	342.88, 434.68	404.33	340.40, 462.60	332.65, 427.55
4h	4-CH_3S C_6H_4	yellow	437.48	406.57	360.56, 467.25	337.61, 429.72
4i	2-Cl C_6H_4	orange	303.80, 437.17	409.79	299.77, 476.56	312.80, 425.07
4j	2-CH_3 C_6H_4	orange	310.62, 435.93	410.33	314.04, 466.94	318.38, 424.76
4k	2-Theinyl	yellow	436.24	424.36	471.91	424.76

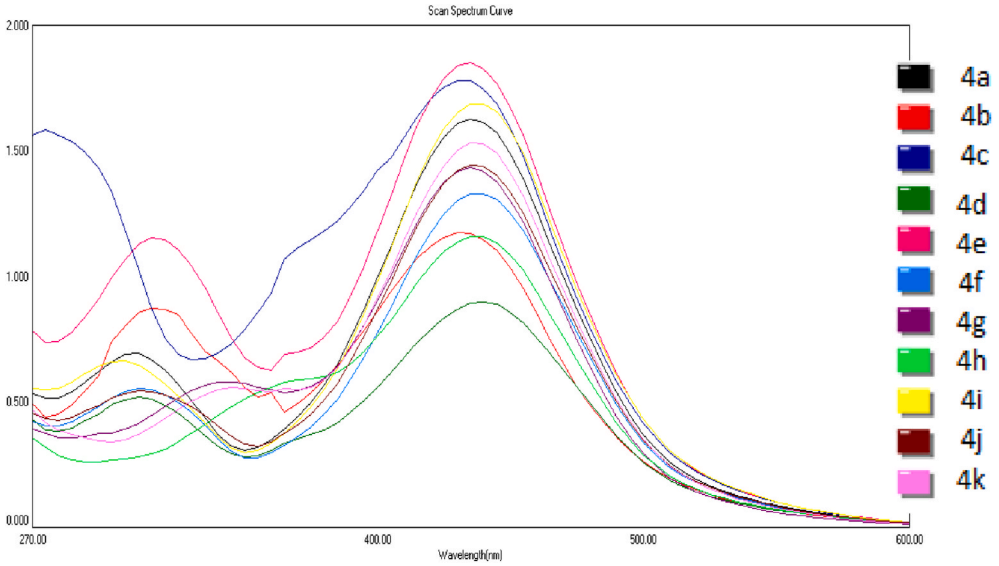

Fig. 2. Absorption Spectra of CAT dye **4a-k** in DMF.

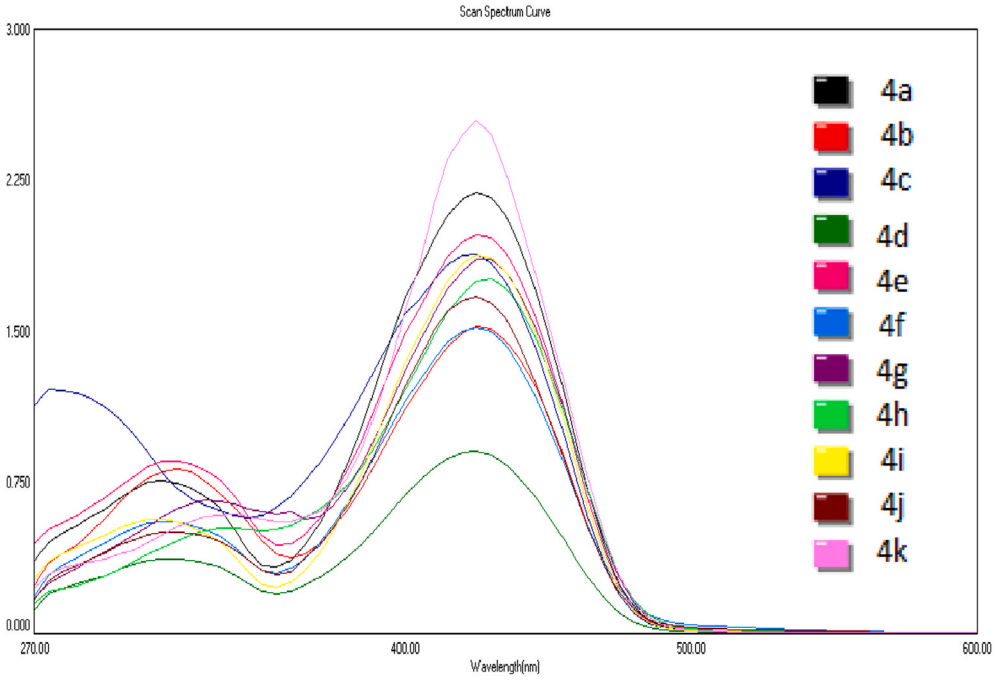

Fig. 3. Absorption Spectra of CAT dye **4a-k** in DMF and 0.1 M HCl.

using Equation (1) [27]. The CAT dyes (**4a-4c** and **4e-4k**) showed relatively moderately to good exhaustion (%) compared onto PET, while dye **4g** displayed excellent exhaustion (%), Table 3.

$$(\%E = \frac{C_1 - C_2}{C_1} 100) \quad 1$$

Attempts are made to apply Hammett equation for 3- and 4- substituents and Taft equation for 2-substituents to know the effect of these substituents on dye exhaustion of dyes **4a-j** on polyester fiber. Hammett plot indicates poor dependence of dye exhaustion on the nature of substituents, however, on removing 3-NO_2 from the plot gives good straight line with negative slope as appeared from their correlation coefficient. The negative slop indicates that electron withdrawing substituents decrease while electron donating substituents increase dye exhaustion. On applying Taft equation for ortho substituents a good correlation coefficient and positive slope of the plot indicating that electron withdrawing increases while that with donating effect decreases dye exhaustion, Table 3. Also the magnitude of ρ* indicates poor effect on dye exhaustion of polyester fiber.

2.6. Color strength

Spectral reflectance measurements on the dyed fabrics, Fig. 5, were carried out using a Jasco - UV/vis/NIR-spectrometer V-570 (1) over 190–2500 nm. The color strength of the dyed fabrics, Table 4, expressed in terms of K/S values at λ_{max} was determined using the Kubelka-Munk [28] Equation (2):

$$K/S = (1-R)^2/2R \quad 2$$

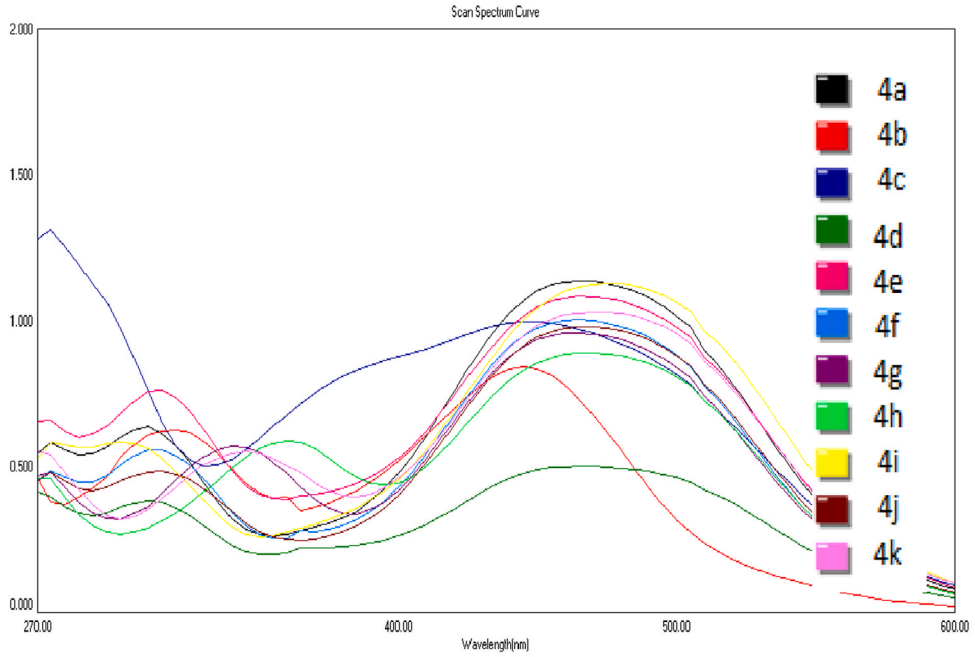

Fig. 4. Absorption Spectra of CAT dye **4a-k** in DMF and 0.1 M NaOH.

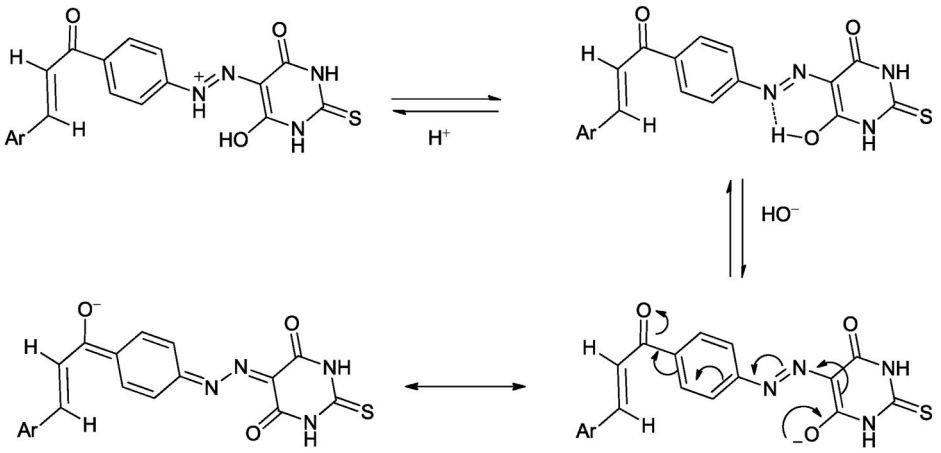

Scheme 3. Protonated and deprotonated structure of CAT dyes **4a-k** in DMF.

Where R is the decimal fraction of the reflection of the dyed fabric; K the absorption coefficient; and S the scattering coefficient.

Data in Table 4 reveals that the color strengths (K/S) of dyed fabrics lie in the same range (0.702–1.769) indicating poor dependence on the nature and position of substituents and this apparently noticed from the hues of the fabrics treated with the CAT azo dyes which vary from yellow to yellowish-orange. Dyed fabric with CAT dye **4i (X = 2-Cl)** showed the high K/S value while CAT dye **4c (X = 3-NO_2)** showed the lowest color strength value.

2.7. Theoretical study and the molecular descriptors

Theoretical analyses have been applied to calculate the tautomerization energy, Table 5, for the three tautomers of CAT dye **4a**. In that way, by using quantum mechanical modeling (DFT method), optimization was performed on the tautomeric forms.

The geometric optimization of dye **4a** showed that the CAT azo-dioxothioxo tautomer **I** is the more stable one and has a lower relative energy ($\Delta E = 0.07$ kcalmol^{-1}) than CAT azo-enol-oxothioxo **III** tautomer which it has a lower energy ($\Delta E = 0.716$ kcalmol^{-1}) than CAT hydrazo-dioxothioxo **II** tautomer, Fig. 6.

2.7.1. Quantum chemical parameters

The DFT method were used to calculate the descriptor parameters [29–32] of both tautomers **II** and **III** as well as to predict the mechanism of dyeing process (see Table 6).

The molecular descriptors were calculated by using B3LYP/6-311G level for investigation of dyeing efficiencies of **4a-k** given in Scheme 1. The calculated molecular descriptors were given in Table 6 at gas phase.

According the Koopman's theorem, as can be seen from Equations (3) and (4), $\mathbf{E_{LUMO}}$ and $\mathbf{E_{HOMO}}$ of any chemical species have been associated with its ionization energy and electron affinity values [29–32], Table 6.

Table 2
Fastness properties of azo disperse CAT dyes (**4a-4c** and **4e-4k**) on polyester fibers (PET).

Dyed polyester fibers	Dye no.	Wash fastness (1–6)			Perspiration fastness (1–6)		Scorch fastness (1–6)	Light fastness (1–6)
		Alt.	SC	SP	acidic	alkaline		
	**4a**	5	3	4–5	3–4	3–4	4–5	4–5
	**4b**	5	3–4	4–5	3	3–4	4–5	4–5
	**4c**	5	3	4–5	3–4	3–4	4–5	4–5
	**4e**	5	3	4–5	3–4	3–4	4–5	4–5
	**4f**	5	3	4–5	3–4	3	4–5	4–5
	**4g**	5	3	4–5	3–4	3–4	4–5	4–5
	**4h**	5	3	4–5	3–4	3–4	4–5	4–5
	**4i**	5	3–4	4–5	3–4	3–4	4–5	4–5
	**4j**	5	3	4–5	3–4	3–4	4–5	4–5
	**4k**	5	3	4–5	3–4	3–4	4–5	4–5

Alt. = alteration, SC = staining on cotton, SP = staining on polyester fiber, PET = polyethylene terephthalate.

Table 3
Dye exhaustion of azo disperse CAT dyes (**4a-4c** and **4e-4k**) on polyester fabrics (PET).

Dye no.	Dye Exhaustion ($\%E = \frac{C_1 - C_2}{C_1} * 100$)	Application of Hammett Equation $\frac{(C_1 - C_2)_X}{(C_1 - C_2)_H}$	σ	Application of Taft Equation $\frac{(C_1 - C_2)_X}{(C_1 - C_2)_{CH_3}}$	σ *
4a	35.71%	1.000	0.00	0.982	0.49
4b	31.21%	0.868	0.78		
4c	63.41%	1.721	0.71		
4e	61.21%	1.482	0.23		
4f	61.82%	1.893	−0.07		
4g	80.15%	2.458	−0.27		
4h	64.51%	1.722	0.00		
4i	49.57%			1.370	2.96
4j	35.46%			1.000	0.00
4k	33.23%	ρ = −0.274 (R^2 = 0.61) 6 points −0.414 (R^2 = 0.99) 5 points (except 3-NO_2)		ρ* = 0.0503 (R^2 = 0.97) 3 points	

$$IP = -E_{HOMO} \quad (3)$$

$$EA = -E_{LUMO} \quad (4)$$

Energy gap **(ΔE)** [33], absolute electronegativity **(χ)**, chemical potential **(μ)**, absolute hardness **(η)** and absolute softness **(σ)** are given by Equations (5-9) [34].

$$\Delta E = E_{HLUMO} - E_{HOMO} \quad (5)$$

$$\chi = \frac{IP + EA}{2} \quad (6)$$

$$\mu = -\chi \quad (7)$$

$$\eta = \frac{IP - EA}{2} \quad (8)$$

$$\sigma = \frac{1}{\eta} \quad (9)$$

Parr et al. have defined electrophilicity index as a measure of energy lowering due to maxima electro flow between donor and acceptor [35].

$$\omega = \frac{\mu^2}{2\eta} \quad (10)$$

The molecular descriptors were calculated by using **B3LYP/6-311G** level for investigation of dyeing efficiencies of **4a-k** given in Scheme 1. The calculated molecular descriptors were given in Table 6 at gas phase.

E_{HOMO} is a parameter associated with the electron donating ability of molecule [36,37]. If the E_{HOMO} increases, electron transfer tendency will increase to the LUMO of appropriate receptor molecules. The molecule having the higher E_{HOMO} indicates the higher dyeing strength. E_{LUMO} is a measure of electron accepting ability of chemical species. E_{LUMO} determines the polarizability of the compound i.e. the ability to be distorted by an electric field, and hence LUMO level receives electrons. Experimental and theoretical studies related to dyeing strength show that increasing of E_{LUMO} decreases the dyeing efficiency of molecules. The separation energy, ΔE is an important parameter as a function of dyeing strength of the molecule. The larger values of the HOMO-LUMO energy gap and chemical hardness will provide low dyeing for fiber. The dyeing efficiencies orders according to ΔE gap will be similar to each other.

Chemical hardness is defined as resistance to electron transfer. The larger values of the chemical hardness will provide low dyeing for fiber.

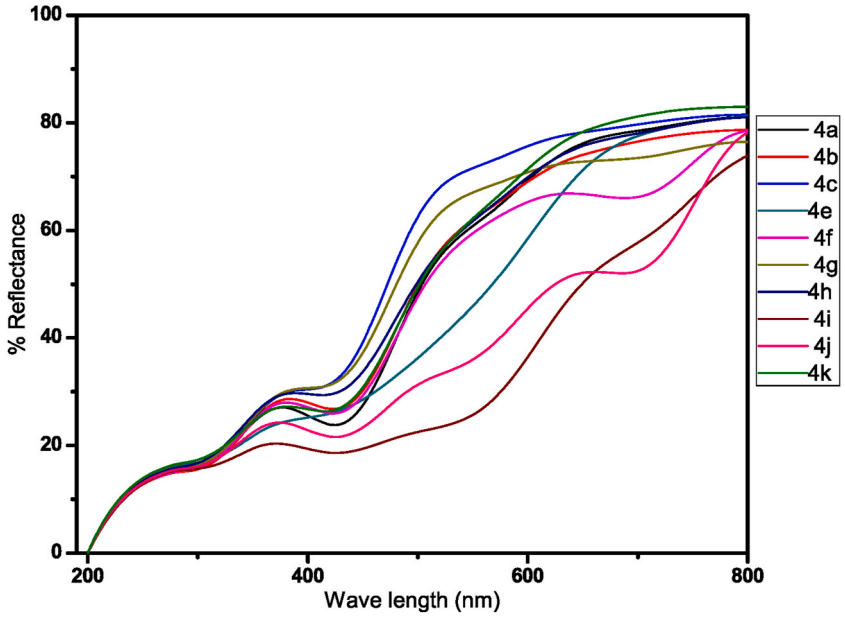

Fig. 5. Reflectance values of the dyed fabrics.

Table 4
Reflectance (%) and color strength (K/S) value of dyed fabrics at λ_{max}.

Dyed Fabric	Reflectance (%)	K/S
4a	24.059	1.198
4b	26.643	1.009
4c	32.786	0.702
4e	26.684	1.007
4f	26.204	1.039
4g	32.149	0.716
4h	30.292	0.802
4i	18.750	1.769
4j	21.328	1.443
4k	27.224	0.972

Table 5
Energy of tautomers I, II, III calculated by the density Functional Theory (DFT) computational analysis [B3LYP/6-311G].

Tautomer		Energy kcal/mol
Azo-dioxothioxo tautomer	**I**	205.008
Hydrazo-dioxothioxo tautomer	**II**	205.794
Azo-enoloxothioxo tautomer	**III**	205.078

The dyeing efficiencies orders according to η will be similar to each other. Softness is the inverse of chemical hardness and represents high dyeing strength. Therefore, soft molecules exhibit high electron donating tendency and high adsorption effect. Exchange of the calculated σ values for these compounds is:

Absolute electronegativity is taken into account as a chemical descriptor in comparison of dyeing strength of fibers. It should be noted that strong colour strength should have low electronegativity values. Because dyeing strength with low electronegativity are tended to give the electron. For a reaction of two systems with different electronegativity the electronic flow will occur from the molecule with the lower electronegativity towards that of higher value until the chemical potentials are equal [38,39]. Chemical potential is the inverse of the electronegativity. Therefore, the dyeing strength increases with increasing of chemical potential. Chemical hardness and softness, chemical potential are known as global reactivity descriptors [35].

Recently, Parr et al. have defined a new descriptor [40]. This parameter is a numeric expression of the global electrophilic power of the molecule that known as electrophilicity index (ω). The electrophilicity index is a descriptor that can represent the dye strength of the chemical species. The global electrophilicity index of the molecule allows quantitative classification of its reactivity [41–45]. The electrophilicity index shows the ability of the electron-accepting ability [46].

Table 6 points out that each parameter exhibits poor effect on dye exhaustion as indicated from its slope value and correlation coefficient. However, parameters $\Delta E(e)$, IP, EA, χ and ω with negative slopes decrease dye exhaustion. While, μ(eV), η, S and μ (D) parameters with positive slopes increase dye exhaustion. Therefore, multiparameters correlation as well as local reactivity may give a concept of the dyeing process.

2.8. Mechanism of dyeing process

^{1}H NMR shows that dyes CAT dye **4a-k** in DMSO existing in the azo enol-oxothioxo III or hydrazo dioxothioxo II tautomers suggesting the formation of hydrogen bonds between the carbonyl group of polyester fiber and the HN< of thiobarbituric moiety of dyes at low temperature Fig. 7 [47].

Transfer of dye onto fiber surface is occurred in slightly basic DMF and slightly acidic medium through exhaustive process without any additives at low-medium temperature with stirring few minutes clockwise followed by stirring anticlockwise. This environments promote vibrational activity and accelerate the migration of the surface of the fiber. Thus a layer is creating called 'Barrier.' If the dye molecules are to reach the fiber surface then the barrier should be broken which is done by agitation. The second step is assembly of dye molecules at the fiber surface leading to adsorption if the dye which is to be distributed is retained by a surface.

When the temperature exceeds the glass transition temperature, the heat motion of the molecular chain turns from a frozen state into violent motion [48]. The diffusion starts because the fiber expands, thus dilating the fiber gap, and allowing the disperse dye molecule to enter the compact fiber molecules, Fig. 8. The final step is reached when the temperature decreases, the pores of material are restored, so that the dye molecules are fixed in the fiber. The disperse dye dyeing is generally based on polyester fiber.

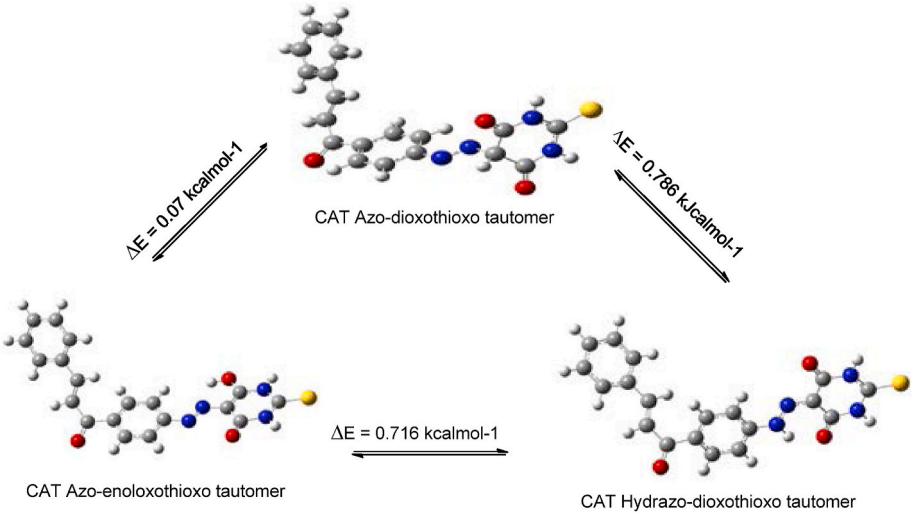

Fig. 6. Geometrical optimization for three tautomers of CAT dye **4a**.

Table 6
Quantum chemical parameters with B3LYP/6-311G level in gas phase of inhibitors.

Cpd	E_{HOMO}	E_{LUMO}	*ΔE(e)*	*IP*	*EA*	*χ*	*μ*(eV)	*η*	*S*	*ω*	*μ* (D)	%E
4a	−0.24385	−0.11934	0.1245	0.2439	0.1193	0.1816	−0.1816	0.0622	16.062	0.2648	7.121	35.71%
4b	−0.25085	−0.13644	0.1144	0.2509	0.1364	0.1936	−0.1936	0.0572	17.480	0.3277	2.719	31.21%
4c	−0.24836	−0.12911	0.1193	0.2484	0.1291	0.1887	−0.1887	0.0596	16.771	0.2987	5.137	63.41%
4d	−0.25341	−0.1342	0.1192	0.2534	0.134	0.1938	−0.1938	0.0596	16.777	0.3150	1.849	–
4e	−0.25215	−0.12987	0.1223	0.2522	0.1298	0.1910	−0.1910	0.0611	16.355	0.2983	2.360	61.21%
4f	−0.24362	−0.11875	0.1249	0.2436	0.1187	0.1812	−0.1811	0.0624	16.016	0.2628	7.581	61.82%
4g	−0.23316	−0.11681	0.1164	0.2332	0.1168	0.1750	−0.1749	0.0581	17.189	0.2631	8.636	80.15%
4h	−0.2296	−0.11851	0.1111	0.2296	0.1185	0.1741	−0.1740	0.0555	18.003	0.2727	7.547	64.51%
4i	−0.24397	−0.12035	0.1236	0.2440	0.1203	0.1822	−0.1821	0.0618	16.178	0.2684	7.5851	49.57%
4j	−0.24405	−0.11944	0.1246	0.2441	0.1194	0.1817	−0.1817	0.0623	16.050	0.2650	6.941	35.46%
4k	−0.23957	−0.12725	0.1123	0.2396	0.1272	0.1834	−0.1834	0.0561	17.806	0.2994	5.402	33.23%
slope			**−0.076**	**−0.336**	**−0.350**	**−0.405**	**+0.405**	**+0.405**	**+0.342**	**−0.096**	**+0.026**	
R^2			**0.0044**	**0.1505**	**0.1367**	**0.1699**	**0.1696**	**0.1696**	**0.0033**	**0.1189**	**0.1083**	

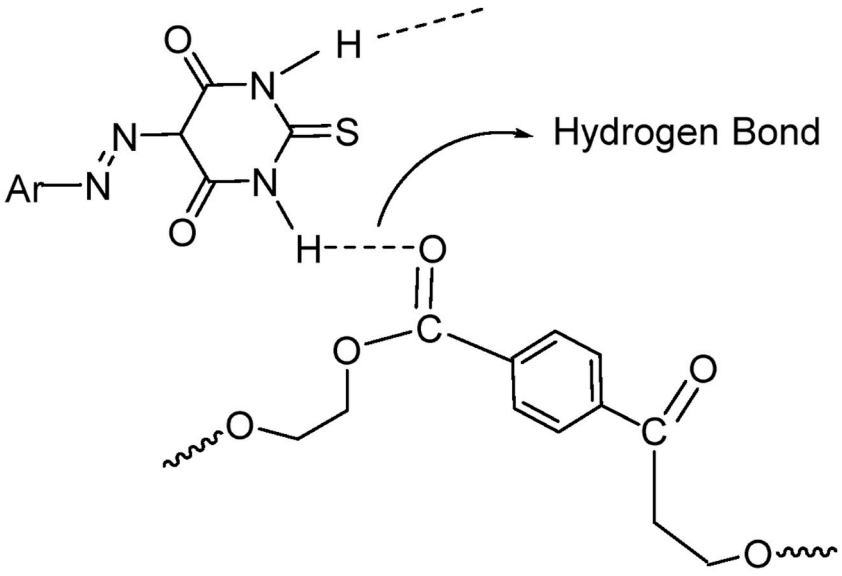

Fig. 7. The bonding mechanisms of polymer and disperse dye.

3. Conclusion

The computational calculation and experimental absorptions of chalcone azo thiobarbituric acid dyes **4a-k** are nearly lie in the same region. The FT-IR spectra of CAT dyes **4a-k** suggested that in the solid phase are predominantly exist in either azo-dioxothioxo tautomer or CAT hydrazo-dioxothioxo. The ^{1}H NMR study suggested the existence of CAT dyes **4a-4c** and **4f-4j** in the azo-enol-oxothioxo tautomer. While,

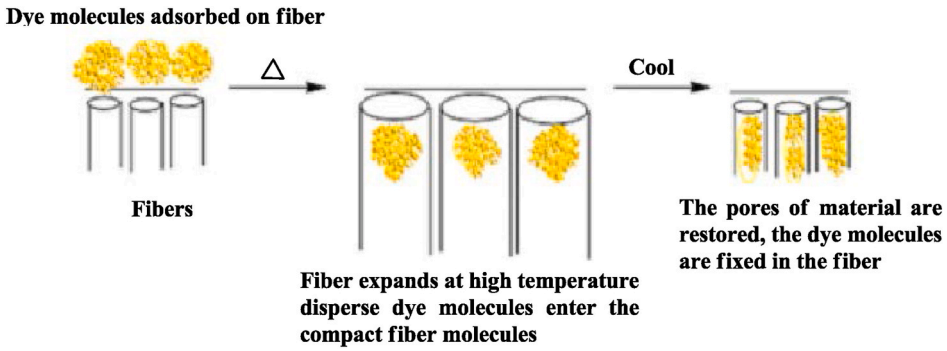

Fig. 8. A schematic image that explain the mechanism of diffusion.

CAT dyes 4d-4e and 4k existed in hydrazo-dioxothioxo tautomer. The effects of the acid and base on the dye solutions showed that the absorption of the dyes in DMF are quite sensitive to pH change. The fastness ratings showed that the disperse CAT dyes (**4a-4c** and **4e-4k**) displayed good to very good fastness levels to washing. The percentage of the individual dye exhaustion on PET (% E) of the CAT dyes (**4a-4c** and **4e-4k**) showed relatively moderately to good exhaustion (%) compared onto PET, while dye **4g** displayed excellent exhaustion (%). The Hammett and Taft relationships indicated poor dependence of dye exhaustion on the nature of substituents. The mechanism of dyeing process was proceeded by three steps. The first step is the transfer of dye onto fiber surface, the second step is assembly of dye molecules at the fiber surface leading to adsorption and the third step was ended by diffusion.

4. Experimental

4.1. Instruments and apparatus

Melting points were determined by MEL-TEMP II melting point apparatus in open glass capillaries. The IR spectra were recorded as potassium bromide (KBr) discs on a Perkin-Elemer FT-IR (Fourier-Transform Infrared Spectroscopy), Faculty of Science, Alexandria University. The NMR spectra were carried out at ambient temperature (~25 °C) on a (JEOL) 500 MHz spectrophotometer using tetramethylsilane (TMS) as an internal standard, NMR Unit, Faculty of Science, Mansoura University. Elemental analyses were analyzed at the Regional Center for Mycology and Biotechnology, Al-Azhar University, Cairo, Egypt. The dyeing process was carried out in Chemical Laboratory of Misr Beida Dyers S.A.E., Alexandria, Egypt.

4.2. General method for synthesis of chalcone 3a-k

4-aminoacetophenone **1** (0.01 mol) was added dropwise (15 min) to a cold solution of sodium hydroxide (0.03 mol) in aqueous ethanol (75 mL, 60%), while stirring at 20 °C. The reaction mixture was stirred for additional 20 min. The desired substituted benzaldehyde **2a-j** and thiophene-2-carbaldehyde **2k** (0.01 mol) was added dropwise (15 min) with stirring for 3–4 h and temperature kept below 20 °C and was left overnight in refrigerator. The separated solid was filtered, washed with cold water and dried, then recrystallized from ethanol to give the corresponding 1-(4-aminophenyl)-3-aryl-propen-1-one **3a-k** [49].

4.3. General method for synthesis of 5-((4-(3-arylacryloyl)phenyl) diazenyl)-2-thioxodihydro-pyrimidine-4,6(1H,5H)-dione 4a-k

A solution of aminochalcones **3a-k** (2.0 mmol) in glacial acetic acid and ethanol mixture (2:1, 6.0 mL) were quickly cooled in an ice-salt bath at 0–5 °C. The mixture was added in portions to a cold solution of nitrosyl sulfuric acid [prepared from sodium nitrite (2.2 mmol, 151.8 mg) and concentrated sulfuric acid (3.0 mL at 0–5 °C). The mixture was stirred for an additional 3 h and the temperature was not exceeded 0–5 °C. The formed diazonium salt solution was added dropwise to thiobarbituric acid (2.0 mmol) dissolved in water contained KOH (2.0 mmol). The resulting solution was vigorously stirred at 0–5 °C for 4 h, while the pH of the reaction mixture was maintained at 7–8 by simultaneous addition of potassium carbonate solution (0.5 M). The progress of the reaction was monitored by TLC and then crude dyes were filtered, washed with hot water for several times.

4.3.1. 5-((4-(3-phenylacryloyl)phenyl)diazenyl)-2-thioxodihydropyrimidine-4,6(1H,5H)-dione (4a)

Yellow crystals, 0.291 g (77%) yield; m.p.319 °C. UV: λ_{max} (DMF) 435 nm and ε_{max} 32580 $mol^{-1}dm^3cm^{-1}$. IR (KBr): 3448 (N–H), 3340 (N–H), 3255 (N–H), 1712 (C═O), 1658 (C═O), 1604 (C═C), 1504 (N═N) and 1342 (C═S) cm^{-1}. ^{1}H NMR (DMSO-d_6, 500 MHz): δ 14.13 (1H, s, OH), 12.50 (2H, s, 2NH), 8.27 (2H, d, J = 8.5 Hz, 2Ar–H), 7.98 (1H, d, J = 15.6 Hz, –CH =), 7.90 (2H, d, J = 3.7 Hz, 2Ar–H), 7.76 (3H, m, 3Ar–H) and 7.46 (3H, m, 3Ar–H) ppm. ^{13}C NMR (APT) (DMSO-d_6, 125 MHz): δ 187.59, 177.69, 145.07, 143.91, 134.72, 134.60, 128.96, 121.88, 120.39 and 116.79 ppm. $C_{19}H_{14}N_4O_3S$ requires: C, 60.31; H, 3.73; N, 14.81% found: C, 60.51; H, 3.27; N, 14.42%

4.3.2. 5-((4-(3-(4-nitrophenyl)acryloyl)phenyl)diazenyl)-2-thioxodihydropyrimidine-4,6(1H,5H)-dione (4b)

Orange crystals, 0.338 g (80%) yield; m.p.294 °C. UV: λ_{max} (DMF) 442.13 nm and ε_{max} 23460 $mol^{-1}dm^3cm^{-1}$. IR (KBr): 3471 (N–H), 3379 (N–H), 3240 (N–H), 3078 (=Sp^2-H), 1705 (C═O), 1658 (C═O), 1597 (C═C), 1504 (N═N) and 1334 (C═S) cm^{-1}. ^{1}H NMR (DMSO-d_6, 500 MHz): δ 13.93 (1H,s, OH), 12.56 (2H, s, 2NH), 8.25 (2H, d, J = 8.8 Hz, 2Ar–H), 8.11 (2H, d, J = 8.7 Hz, 2Ar–H), 8.06 (1H, d, J = 15.6 Hz, =CH-), 7.94 (2H, d, J = 8.6 Hz, 2Ar–H), 7.82 (1H, d, J = 15.6 Hz, =CH-) and 7.77 (2H, d, J = 8.7 Hz, Ar–H) ppm. ^{13}C NMR (APT) (DMSO-d_6, 125 MHz): δ 187.38, 177.69, 154.27, 148.07, 141.24, 140.97, 134.15, 130.76, 129.92, 126.67, 124.96, 123.92 and 120.50 ppm. $C_{19}H_{13}N_5O_5S$ requires: C, 53.90; H, 3.09; N, 16.54% found: C, 54.11; H, 3.28; N, 16.85%

4.3.3. 5-((4-(3-(3-nitrophenyl)acryloyl)phenyl)diazenyl)-2-thioxodihydropyrimidine-4,6(1H,5H)-dione (4c)

Orange crystals, 0.329 g (78%) yield; m.p.270 °C. UV: λ_{max} (DMF) 432.51 nm and ε_{max} 35640 $mol^{-1}dm^3cm^{-1}$. IR (KBr): 3471 (N–H), 3340 (N–H), 3232 (N–H), 3078 (=Sp^2-H), 1705 (C═O), 1643 (C═O), 1604 (C═C), 1519 (N═N) and 1342 (C═S) cm^{-1}. ^{1}H NMR (DMSO-d_6, 500 MHz): δ 13.87 (1H, s, OH), 12.57 (2H, s, 2NH), 8.21 (2H, m, =CH- and Ar–H), 7.97 (2H, d, J = 8.5 Hz, 2Ar–H), 7.86 (1H, d, J = 15.6 Hz, =CH-) and 7.73 (5H, m, 5Ar–H) ppm. ^{13}C NMR (APT) (DMSO-d_6, 125 MHz): δ 187.42, 177.79, 154.17, 141.29, 136.64, 134.83, 134.23, 131.43, 125.29, 125.03, 124.11, 122.63, 120.57 and 112.73 ppm. $C_{19}H_{13}N_5O_5S$ requires: C, 53.90; H, 3.09; N, 16.54% found: C, 54.12; H, 3.27; N,

16.76%

4.3.4. 5-((4-(3-(4-chlorophenyl)acryloyl)phenyl)diazenyl)-2-thioxodihydropyrimidine-4,6(1H,5H)-dione (4d)

Yellow crystals, 0.288 g (70%) yield; m.p.304 °C. UV: λ_{max} (DMF) 439.65 nm and ε_{max} 17980 $mol^{-1}dm^3cm^{-1}$. IR (KBr): 3425 (N–H), 3255 (2 N–H), 3079 (=Sp2-H), 1712 (C═O), 1658 (C═C), 1604 (C═C), 1504 (N═N) and 1350 (C═S) cm^{-1}. ^{1}H NMR (DMSO-d_6, 500 MHz): δ 12.80 (3H, s, 3NH), 8.26 (2H, d, J = 8.6 Hz, 2Ar–H), 8.01 (1H, d, J = 15.5 Hz, –CH =), 7.94 (2H, d, J = 8.4 Hz, 2Ar–H), 7.72 (3H, m, 2Ar–H and –CH =) and 7.53 (2H, d, J = 8.4 Hz, 2Ar–H) ppm. ^{13}C NMR (APT) (DMSO-d_6, 125 MHz): δ 187.50, 154.25, 142.23, 135.05, 134.31, 133.76, 130.63, 130.45, 128.96, 122.69, 120.23, 117.37 and 112.71 ppm. $C_{19}H_{13}ClN_4O_3S$ requires: C, 55.28; H, 3.17; N, 13.57% found: C, 55.49; H, 3.42; N, 13.75%

4.3.5. 5-((4-(3-(4-bromophenyl)acryloyl)phenyl)diazenyl)-2-thioxodihydropyrimidine-4,6(1H,5H)-dione (4e)

Yellow crystals, 0.356 g (78%) yield; m.p.320 °C. UV: λ_{max} (DMF) 434.37 nm and ε_{max} 37060 $mol^{-1}dm^3cm^{-1}$. IR (KBr): 3456 (N–H), 3255 (N–H), 3109 (N–H), 3000 (=Sp^2-H), 1712 (C═O), 1658 (C═O), 1604 (C═C), 1504 (N═N) and 1350 (C═S) cm^{-1}. ^{1}H NMR (DMSO-d_6, 500 MHz): δ 12.88 (3H, s, 3NH), 8.27 (2H, d, J = 8.7 Hz, 2Ar–H), 8.02 (1H, d, J = 15.5 Hz, –CH =), 7.87 (2H, d, J = 8.4 Hz, 2Ar–H), 7.75 (2H, d, J = 8.7 Hz, 2Ar–H), 7.72 (1H, d, J = 15.7 Hz, –CH =) and 7.66 (2H, d, J = 8.4 Hz, 2Ar–H) ppm. ^{13}C NMR (APT) (DMSO-d_6, 125 MHz): δ 187.47, 177.72, 173.20, 142.43, 134.41, 134.05, 131.89, 130.85, 130.54, 123.99, 122.67, 120.34 and 116.99 ppm. $C_{19}H_{13}BrN_4O_3S$ requires: C, 49.90; H, 2.87; N, 12.25% found: C, 50.15; H, 3.11; N, 12.49%

4.3.6. 5-((4-(3-(3-methylphenyl)acryloyl)phenyl)diazenyl)-2-thioxodihydropyrimidine-4,6(1H,5H)-dione (4f)

Yellow crystals, 0.297 g (76%) yield; m.p.296 °C. UV: λ_{max} (DMF) 437.43 nm and ε_{max} 26600 $mol^{-1}dm^3cm^{-1}$. IR (KBr): 3390 (N–H), 3248 (N–H), 3109 (N–H), 2862 (-Sp^3-H), 1712 (C═O), 1658 (C═O), 1604 (C═C), 1504 (N═N) and 1350 (C═S) cm^{-1}. ^{1}H NMR (DMSO-d_6, 500 MHz): δ 14.14 (1H, s, OH), 12.52 (2H, s, 2NH), 8.27 (2H, d, J = 8.0 Hz, 2Ar–H), 7.95 (1H, d, J = 15.5 Hz, –CH =), 7.75 (5H, m, 4Ar–H and –CH =), 7.34 (1H, t, J = 7.2 Hz, Ar–H), 7.27 (1H, d, J = 6.8 Hz, Ar–H) and 2.36 (3H, s, CH_3) ppm. ^{13}C NMR (APT) (DMSO-d_6, 125 MHz): δ 187.58, 177.71, 145.05, 144.10, 138.23, 134.66, 131.44, 130.57, 129.21, 128.87, 126.46, 121.64, 120.39, 116.81 and 20.93 ppm. $C_{20}H_{16}N_4O_3S$ requires: C, 61.21; H, 4.11; N, 14.28% found: C, 61.46; H, 4.34; N, 14.07%

4.3.7. 5-((4-(3-(4-methoxyphenyl)acryloyl)phenyl)diazenyl)-2-thioxodihydropyrimidine-4,6(1H,5H)-dione (4g)

Orange crystals, 0.302 g (74%) yield; m.p.319 °C. UV: λ_{max} (DMF) 434.68 nm and ε_{max} 28680 $mol^{-1}dm^3cm^{-1}$. IR (KBr): 3441 (N–H), 3309 N–H), 3109 (N–H), 2924 (-Sp^3-H), 1712 (C═O), 1658 (C═O), 1597 (C═C), 1504 (N═N) and 1350 (C═S) cm^{-1} .^{1}HNMR (DMSO-d_6, 500 MHz): δ 14.17 (1H, s, OH), 12.52 (2H, s, 2NH), 8.25 (2H, d, J = 8.4 Hz, 2Ar–H), 7.85 (3H, m, 2Ar–H and –CH =), 7.74 (3H, m, 2Ar–H and –CH =), 7.02 (2H, d, J = 8.4 Hz, 2Ar–H) and 3.82 (3H, s, OCH_3) ppm. ^{13}C NMR (APT) (DMSO-d_6, 125 MHz): δ 187.41, 177.68, 161.40, 134.91, 130.88, 130.40, 127.37, 120.28, 119.32, 116.78, 114.43 and 55.41 ppm. $C_{20}H_{16}N_4O_4S$ requires: C, 58.81; H, 3.95; N, 13.72% found: C, 59.07; H, 4.18; N, 14.01%

4.3.8. 5-((4-(3-(4-methylthiophenyl)acryloyl)phenyl)diazenyl)-2-thioxodihydropyrimidine-4,6(1H,5H)-dione (4h)

Orange crystals, 0.305 g (72%) yield; m.p.315 °C. UV: λ_{max} (DMF) 437.48 nm and ε_{max} 23180 $mol^{-1}dm^3cm^{-1}$. IR (KBr): 3425 (N–H), 3278 (N–H), 3101 (N–H), 2916 (-Sp^3-H), 1705 (C═O), 1666 (C═O), 1597 (C═C), 1496 (N═N) and 1342 (C═S) cm^{-1}. ^{1}H NMR (DMSO-d_6, 500 MHz): δ 13.98 (1H, s, OH), 12.54 (2H, s, 2NH), 8.26 (2H, d, J = 7.9 Hz, 2Ar–H), 7.93 (1H, d, J = 15.5 Hz, –CH =), 7.83 (2H, d, J = 7.6 Hz, 2Ar–H), 7.75 (2H, d, J = 8.0 Hz, 2Ar–H), 7.71 (1H, d, J = 15.9 Hz, –CH =), 7.31 (2H, d, J = 7.6 Hz, 2Ar–H) and 2.52 (s, 3H, SCH 3) ppm. ^{13}C NMR (APT) (DMSO-d_6, 125 MHz): δ 187.47, 177.70, 145.03, 143.57, 142.19, 134.79, 131.20, 130.66, 129.47, 125.55, 120.68, 120.34, 116.82 and 14.17 ppm. $C_{20}H_{16}N_4O_3S_2$ requires: C, 56.59; H, 3.80; N, 13.20% found: C, 56.84; H, 3.98; N, 13.49%

4.3.9. 5-((4-(3-(2-chlorophenyl)acryloyl)phenyl)diazenyl)-2-thioxodihydropyrimidine-4,6(1H,5H)-dione (4i)

Orange crystals, 0.33 g (80%) yield; m.p.290 °C. UV: λ_{max} (DMF) 437.17 nm and ε_{max} 33740 $mol^{-1}dm^3cm^{-1}$. IR (KBr): 3425 (N–H), 3248 (N–H), 3093 (N–H), 3000 (=Sp^2-H), 1712 (C═O), 1658 (C═O), 1604 (C═C), 1496 (N═N) and 1350 (C═S) cm^{-1}. ^{1}H NMR (DMSO-d_6, 500 MHz): δ 14.04 (1H, s, OH), 12.54 (2H, s, 2NH), 8.28 (2H, d, J = 8.2 Hz, 2Ar–H), 8.23 (1H, d, J = 6.4 Hz, Ar–H), 8.03 (2H, m, 2Ar–H), 7.77 (2H, d, J = 8.2 Hz, 2Ar–H), 7.57 (1H, d, J = 6.9 Hz, Ar–H) and 7.48 (2H, m, 2Ar–H) ppm. ^{13}C NMR (APT) (DMSO-d_6, 125 MHz): δ 187.50, 177.77, 145.38, 138.33, 134.40, 134.25, 132.30, 132.11, 130.70, 130.06, 128.64, 127.72, 124.62, 120.47 and 116.82 ppm. $C_{19}H_{13}ClN_4O_3S$ requires: C, 55.28; H, 3.17; N, 13.57% found: C, 55.49; H, 3.42; N, 13.34%

4.3.10. 5-((4-(3-(2-methylphenyl)acryloyl)phenyl)diazenyl)-2-thioxodihydropyrimidine-4,6(1H,5H)-dione (4j)

Orange crystals, 0.313 g (80%) yield; m.p.282 °C. UV: λ_{max} (DMF) 435.93 nm and ε_{max} 28880 $mol^{-1}dm^3cm^{-1}$. IR (KBr): 3448 (N–H), 3147 (2 N–H), 3055 (=Sp^2-H) 2916 (-Sp^3-H), 1659 (C═O), 1651 (C═O), 1589 (C═C), 1504 (N═N) and 1334 (C═S) cm^{-1}. ^{1}H NMR (DMSO-d_6, 500 MHz): δ 14.17 (1H, s, OH), 12.54 (2H, s, 2NH), 8.26 (1H, d, J = 7.7 Hz, 2Ar–H), 7.99 (2H, d, J = 14.6 Hz, 2Ar–H), 7.85 (1H, d, J = 15.3 Hz, –CH =), 7.76 (2H, d, J = 7.7 Hz, 2Ar–H), 7.32 (3H, m, 2Ar–H and CH =) and 2.44 (3H, s, CH_3) ppm. ^{13}C NMR (APT) (DMSO-d_6, 125 MHz): δ 187.63, 177.69, 140.89, 138.08, 134.60, 133.31, 130.83, 130.56, 130.44, 126.92, 126.40, 122.75, 120.37, 116.82 and 19.37 ppm. $C_{20}H_{16}N_4O_3S$ requires: C, 61.21; H, 4.11; N, 14.28% found: C, 60.97; H, 4.34; N, 14.50%

4.3.11. 5-((4-(3-(thiophen-2-yl)acryloyl)phenyl)diazenyl)-2-thioxodihydropyrimidine-4,6(1H,5H)-dione (4k)

Yellow crystals, 0.307 g (80%) yield; m.p.275 °C. UV: λ_{max} (DMF) 436.24 nm and ε_{max} 30640 $mol^{-1}dm^3cm^{-1}$. IR (KBr): 3417 (N–H), 3248 (N–H), 3101 (N–H), 1705 (C═O), 1658 (C═O), 1589 (C═C), 1504 (N═N) and 1346 (C═S) cm^{-1}. ^{1}H NMR (DMSO-d_6, 500 MHz): δ 12.83 (3H, s, 3NH), 8.18 (2H, d, J = 8.6 Hz, 2Ar–H), 7.91 (1H, d, J = 15.3 Hz, –CH =), 7.79 (1H, d, J = 5.0 Hz, thienyl-H), 7.70 (3H, m, 2Ar–H and thienyl-H), 7.60 (1H, d, J = 15.3 Hz, –CH =) and 7.19 (1H, t, thienyl-H) ppm. ^{13}C NMR (APT) (DMSO-d_6, 125 MHz): δ 159.06, 156.52, 143.74, 135.47, 134.94, 132.65, 130.56, 130.44, 129.22, 129.07, 128.66, 128.61, 128.44, 128.41, 126.80, 122.36 and 115.18 ppm. $C_{17}H_{12}N_4O_3S_2$ requires: C, 53.11; H, 3.15; N, 14.57% found: C, 53.28; H, 3.41; N, 14.39%

4.4. Dyeing process

Disperse Cat dyes **4a-4c** and **4e-4k** were applied to polyester fiber (PET), using high temperature dyeing method (HT) at 130 °C with a material to liquor ratio of 1:20. 2% Dye was used for dying (calculated on weight of the fiber). The dye was dissolved in 20 mL DMF, while pH of the dye bath was adjusted to 4.5 using aqueous acetic acid and the polyester fibres were added. Dyeing was performed by raising the dye bath temperature to 130 °C under pressure in a dyeing machine at a rate of 3 °C/min, holding at this temperature for 60 min and cooling to 50 °C. After dyeing, the fiber was thoroughly washed and subjected to surface reduction clearing [(1 g NaOH + 1 g sodium hydrosulphite)/L. The samples were heated in this solution for 10 min at 60 °C and then thoroughly washed and air-dried.

Role of each author

Alaa Z. Omar: Designed the research; performed the experimental work; analyzed the data; wrote the manuscript; revised the manuscript; all the authors discussed, edited and approved the final revision. **Mona N. Mahmoud:** performed the experimental work; analyzed the data; wrote the manuscript; all the authors discussed, edited and approved the final revision. **Samir K. El-Sadany:** Designed the research; wrote the manuscript; revised the manuscript; all the authors discussed, edited and approved the final revision. **Ezzat A. Hamed:** Designed the research; wrote the manuscript; revised the manuscript; all the authors discussed, edited and approved the final revision. **Mohamed A. El-atawy:** Designed the research; performed the experimental work; analyzed the data; wrote the manuscript; revised the manuscript; all the authors discussed, edited and approved the final revision

Declaration of competing interest

The authors declare that they have no known competing financial interests or personal relationships that could have appeared to influence the work reported in this paper.

Acknowledgements

The authors are thankful to Misr Beida Dyers for support of this research and providing the financial assistance through dyeing process.

Appendix A. Supplementary data

Supplementary data to this article can be found online at https://doi.org/10.1016/j.dyepig.2020.108887.

References

[1] Matijević BM, Vaštag ĐĐ, Apostolov SL, Assaleh F, Marinković AD, Mijin DŽ. Solvatochromism of thiouracil azo dyes. J Solut Chem 2016;45:885–906.
[2] Parekh NM, Maheria KC. Dyeing performance of heterocyclic monoazo dyes based on 3-amino-1*H*-pyrazolone[3,4-*b*]quinoline derivatives on various fibers. Arch Appl Sci Res 2011;3:359–65.
[3] Kareem SM. Synthesis, Characterization and dying performance studies of some azo dyes derived from m-phenylenediamine. J Pure Appl Sci 2017;28:148–57.
[4] Salem MA, Marzouk MI, Mashaly HM. Synthesis of pharmacological dyes and their application on synthetic fabrics. Color Technol 2015;131:288–97.
[5] Kınalı S, Demirci S, Çalışır Z, Kurt M, Ataç A. DFT, FT-IR, FT-Raman and NMR studies of 4-(substituted phenylazo)-3,5-diacetamido-1*H*-pyrazoles. J Mol Struct 2011;993:254–8.
[6] Al-Obaidi NS, Sattar ODA, Hadi FF, Ali AS, Zaki BT. Synthesis and characterization of some azo dyes derived from 4-aminoacetophenone, 1, 4 phenylene diamine and studying its dyeing performance and antibacterial activity. J Biochem Technol 2018;9:33.
[7] Elmaaty TA, Elnagar K, Hassan S, Gamal H. Antibacterial activity and dyeing characteristics of some azo-pyazole disperse dyes using eco-friendly ultrasound energy for PET fabric. Int J Sci Eng Res 2014;5:1156–61.
[8] Al-Etaibi A, Kamel MM, El-Apasery MA. Synthesis and applications of new aminothienopyridazines disperse dyes on polyester fabric. Int J Curr Microbiol Appl Sci 2014;3:826–32.
[9] Kumar R, Raghuvanshi K, Verma RK, Singh MS. Application of cyclic-1,3-diketones in domino and multicomponent reactions: facile route to highly functionalized chromeno[2,3-*d*]pyrimidinones and diazabenzo[*b*]fluorenones under solvent-free conditions. Tetrahedron Lett 2010;51:5933–6.
[10] Khoshkholgh MJ, Balalaie S, Bijanzadeh HR, Rominger F, Gross JH. Synthesis of novel annulated uracils via domino Knoevenagel-hetero-Diels–Alder reaction in aqueous media. Tetrahedron Lett 2008;49:6965–8.
[11] Sweidan K, Al-Sheikh A, Sweileh B, Sunjuk M, Kuhn N. Synthesis of phosphorus, arsenic and antimony ylides containing the 1, 3-dimethyl-2,4,6(1*H*, 3*H*, 5*H*)-pyrimidinetrione fragments. Lett Org Chem 2009;6:1–3.
[12] Blythin D.J., 2,4-[1H, 3H, 5H]-(1)-Benzopyrano-[2,3-*d*]-pyrimidinediones and their use as anti-allergy agents, Google Patents, 1981.
[13] Kidwai M, Venkataramanan R, Dave B. Antifungal activity of solventlessly synthesized organomercurials. Met Base Drugs 2002;8:283–5.
[14] Kidwai M, Thakur R, Mohan R. Ecofriendly synthesis of novel antifungal (thio) barbituric acid derivatives. Acta Chim Slov 2005;52:88–92.
[15] Ashkinazi R. Salts of 5,5-(arylidenebisbarbituric and 5,5-(Arylidene-bis(2-Thiobarbituric) acids and 5,5-(arylidenebis(2-thiobarbituric) acids having an antibacterial, anti-chlamydial, antiviral and immuno-modulating activity. Int Patent WO 1999;99:25699.
[16] Fellahi Y, Dubois P, Agafonov V, Moussa F, Ombetta-Goka J-É, Guenzet J, Frangin Y. Synthesis and characterization of a new pyrimidine derivative: 5-[1-phenyl-2-(3-chlorophenyl)ethyl]-2, 4, 6-trichloropyrimidine. Bull Soc Chim Fr 1996;9:869–74.
[17] Oliva A., De Cillis G., Grams F., Livi V., Zimmermann G., Menta E. and Krell H.-W., Barbituric acid derivatives with antimetastatic and antitumor activity, Google Patents, 2002.
[18] Noroozi PN, Khalafy J, Akbari DK, Rastgar S, Malekpoor Z, Mohammadzadeh M. Tautomeric behaviors of 5-arylazobarbituric acids in different concentrations. J Iran Chem Res 2009;2:133–44.
[19] Silverstein RM, Bassler GC. Spectrometric identification of organic compounds. J Chem Educ 1962;39:546.
[20] Asiri AM, Marwani HM, Alamry KA, Al-Amoudi MS, Khan SA, El-Daly SA. Green synthesis, characterization, photophysical and electrochemical properties of bis-chalcones. Int J Electrochem Sci 2014;9:799–809.
[21] Lutoshkin MA, Kazachenko AS. Assessment of various density functionals and solvation models to describe acid-base, spectral and complexing properties of thiobarbituric and barbituric acids in aqueous solution. J Comput Methods Sci Eng 2017;17:851–63.
[22] Stuckey R. The ultra-violet absorption spectra of barbituric acid and its 1-methyl and 1: 3-dimethyl derivatives. Q J Pharm Pharmacol 1940;13:312.
[23] Satam MA, Raut RK, Sekar N. Fluorescent azo disperse dyes from 3-(1,3-benzothiazol-2-yl)naphthalen-2-ol and comparison with 2-naphthol analogs. Dyes Pigments 2013;96:92–103.
[24] Shukla S, Mathur MR. Low-temperature ultrasonic dyeing of silk. J Soc Dye Colour 1995;111:342–5.
[25] Fang S, Feng G, Guo Y, Chen W, Qian H. Synthesis and application of urethane-containing azo disperse dyes on polyamide fabrics. Dyes Pigments 2020;176:108225–37.
[26] Cai J, Jiang H, Chen W, Cui Z. Design, synthesis, characterization of water-soluble indophenine dyes and their application for dyeing of wool, silk and nylon fabrics. Dyes Pigments 2020:108385–98.
[27] Wang Z, Wu ZW. A study of novel bisazo reactive red dyes with good wet fastness. Color Technol 2009;125:216–21.
[28] Soliman H, Yahia I. Synthesis and technical analysis of 6-butyl-3-[(4-chlorophenyl) diazenyl]-4-hydroxy-2H-pyrano [3,2-*c*] quinoline-2,5 (6*H*)-dione as a new organic semiconductor: structural, optical and electronic properties. Dyes Pigments 2020;176:108199–211.
[29] Koopmans T. Ordering of wave functions and eigenenergies to the individual electrons of an atom. Physica 1933;1:104–13.
[30] Kaya S, Kariper SE, Ungördü A, Kaya C. Effect of some electron donor and electron acceptor groups on stability of complexes according to the principle of HSAB. J New Result Sci 2014;3. 1-1.
[31] Alexander D, Moccari A. Evaluation of corrosion inhibitors for component cooling water systems. Corrosion Sci 1993;49:921–8.
[32] Sastri V, Perumareddi J. Molecular orbital theoretical studies of some organic corrosion inhibitors. Corrosion Sci 1997;53:617–22.
[33] Kohn W, Sham L. Quantum density oscillations in an inhomogeneous electron gas. Phys Rev 1965;137:A1697.
[34] Pearson RG. Absolute electronegativity and hardness: application to inorganic chemistry. Inorg Chem 1988;27:734–40.
[35] Parr RG, Szentpaly Lv, Liu S. Electrophilicity index. J Am Chem Soc 1999;121:1922–4.
[36] Jesus AL, Tomé LI, Eusébio MES, Rosado MT, Redinha J. Hydration of cyclohexylamines: CPCM calculation of hydration gibbs energy of the conformers. J Phys Chem A 2007;111:3432–7.
[37] Udhayakala P, Samuel AM, Rajendiran T, Gunasekaran S. Quantum chemical study on inhibitory action of some substituted 1, 3, 4-oxadiazoles on mild steel. Der Pharm Lett 2013;5:272–83.
[38] Martinez S. Inhibitory mechanism of mimosa tannin using molecular modeling and substitutional adsorption isotherms. Mater Chem Phys 2003;77:97–102.
[39] Parthasarathi R, Subramanian V, Roy DR, Chattaraj P. Electrophilicity index as a possible descriptor of biological activity. Bioorg Med Chem 2004;12:5533–43.
[40] Parthasarathi R, Padmanabhan J, Subramanian V, Maiti B, Chattaraj P. Chemical reactivity profiles of two selected polychlorinated biphenyls. J Phys Chem A 2003;107:10346–52.
[41] Thanikaivelan P, Subramanian V, Rao JR, Nair BU. Application of quantum chemical descriptor in quantitative structure activity and structure property relationship. Chem Phys Lett 2000;323:59–70.
[42] Parthasarathi R, Padmanabhan J, Elango M, Subramanian V, Chattaraj P. Intermolecular reactivity through the generalized philicity concept. Chem Phys Lett 2004;394:225–30.
[43] Parthasarathi R, Padmanabhan J, Subramanian V, Maiti B, Chattaraj P. Toxicity analysis of 33'44'5-pentachlorobiphenyl through chemical reactivity and selectivity profiles. Curr Sci 2004;86:535–9.
[44] Parthasarathi R, Padmanabhan J, Subramanian V, Sarkar U, Maiti B, Chattaraj P. Toxicity analysis of benzidine through chemical reactivity and selectivity profiles: a DFT approach. Internet Electron J Mol Des 2003;2:798–813.
[45] Obi-Egbedi N, Obot I, El-Khaiary MI. Quantum chemical investigation and statistical analysis of the relationship between corrosion inhibition efficiency and molecular structure of xanthene and its derivatives on mild steel in sulphuric acid. J Mol Struct 2011;1002:86–96.
[46] Politzer P, Truhlar DG. Chemical applications of atomic and molecular electrostatic potentials: reactivity, structure, scattering, and energetics of organic, inorganic, and biological systems. Springer Science & Business Media; 2013.

[47] Li M-J, Huang Y-H, Ju A-Q, Yu T-S, Ge M-Q. Synthesis and characterization of azo dyestuff based on bis(2-hydroxyethyl)terephthalate derived from depolymerized waste poly (ethylene terephthalate) fibers. Chin Chem Lett 2014;25:1550–4.
[48] Lee M-J, Ho C-C, Lin H-m, Wang P-y, Lu J-s. Solubility of Disperse Red 82 and modified Disperse Yellow 119 in supercritical carbon dioxide or nitrous oxide with ethanol as a cosolvent. J Supercrit Fluids 2014;95:258–64.
[49] Rashid U, Sultana R, Shaheen N, Hassan SF, Yaqoob F, Ahmad MJ, Iftikhar F, Sultana N, Asghar S, Yasinzai M. Structure based medicinal chemistry-driven strategy to design substituted dihydropyrimidines as potential antileishmanial agents. Eur J Med Chem 2016;115:230–44.